Article:
Sanders, L, Hu, X, Mavredaki, E et al. (3 more authors) (2014) Assessment of combined scale/corrosion inhibitors - A combined jar test/bubble cell. Journal of Petroleum Science and Engineering, 118. 126 - 139. ISSN 0920-4105

https://doi.org/10.1016/j.petrol.2014.04.008

Assessment of combined scale/corrosion inhibitors – A combined jar test/bubble cell

Laura Sanders, Xinming Hu, Eleftheria Mavredaki, Violette Eroini, Richard Barker, Anne Neville

Institute of Engineering Thermofluids, Surfaces and Interfaces, School of Mechanical Engineering, University of Leeds, Leeds LS2 9JT, United Kingdom

Abstract

The formation of calcium carbonate scale and the occurrence of CO_2 corrosion are both widespread phenomena observed within pipework during oil and gas production. The most common form of treatment for both processes is the application of chemical inhibition through corrosion and/or scale inhibitors. Surface scaling of pipework rarely occurs in environments where no corrosion exists, yet techniques used to develop and assess the performance of scale inhibitors tend to focus on assessing and reducing solely bulk/surface scaling, without affording consideration towards corrosion, whilst corrosion inhibitors are frequently evaluated in non-scaling environments. Furthermore, both chemicals tend to be evaluated independently meaning that any potential antagonistic effects between the chemicals can go unrecognised.

This paper addresses this very issue by presenting a unique setup and methodology to enable the occurrence of scale and corrosion to be monitored simultaneously in a CO_2-saturated environment in the presence and absence of combined scale and corrosion inhibitors. The test cell focuses on evaluating four key parameters which are quantified either throughout the duration of the test, or from the implementation of post-test surface analysis techniques.

The multiple assessment of (i) bulk scale precipitation, (ii) surface scaling, (iii) general corrosion and (iv) localised corrosion permits a full assessment of the chemical blends propensity to mitigate both scaling and corrosion. Non-inhibited tests were initially conducted at 60 °C to form a baseline for comparison. Four combined scale/corrosion inhibitors were subsequently used at low concentrations in order to understand their mechanisms and highlight any competitive effect which existed in reducing either scale or corrosion. The results demonstrate that the methodology implemented is effective at assessing the efficiency of combined inhibitors in reducing both corrosion and scale in environments where both processes occur simultaneously. The limitations of conducting solely bulk scaling or corrosion tests in non-scaling environments are discussed relative to the results obtained in this work. The results of each individual inhibitor are discussed and

markedly different behaviour is observed according to the concentration administered, as well as the particular blend of chemicals applied.

Keywords: scale; corrosion; combined inhibitors; calcium carbonate

1. Introduction

Scaling and corrosion processes can result in serious implications in oil and gas production through the blockage of production equipment, the deterioration of metallic surfaces and/or the loss of capacity for thermal exchange (Touir et al., 2009).

The formation of sparingly soluble, inorganic material is referred to as “scaling”. The deposition of scale in different locations of oil and gas facilities can result in a decrease in the internal diameter and subsequent choking of the production from the reservoir. The cost of scale has been estimated at more than USD $1.5 billion per year (Frenier and Ziauddin, 2008).

Corrosion is the principal cause of damage to metal alloys in wells and production facilities (Chilingar et al., 2008) given that corrodible surfaces are ubiquitous throughout production, transport and refining systems (Becker, 1998). Corrosion can be a major factor in hydrocarbon leaks which are the most common incidents encountered during production. The costs are estimated in industry at $276 billion per year (Lyons and Plisga, 1996 and Koch et al., 2001). Chemical techniques, such as the use of inhibitors, are mainly applied as individual treatments for scale or corrosion since inhibitors have been proved to be successful and cost effective (Garverick, 1994 and Chilingar et al., 2008). Inhibitors can act as surface active component and can form a protective layer on the substrate which modifies the properties of the surface (Nesic et al., 2001 and Sun and Nesic, 2008).

According to the increasingly stringent legislation to decrease the human impact on the environment, methodologies have been developed. For the North-East region, it is the convention for the protection of the marine environment (OSPAR convention) which is in charge of protecting the shared maritime areas (Ospar, 2003). The convention′s work is organised under six strategies: Biodiversity and Ecosystem Strategy, Eutrophication Strategy, Hazardous Substances Strategy, Offshore Industry Strategy, Radioactive Substance Strategy and a Strategy for the Joint Assessment and Monitoring Programme. Since June 2000, OSPAR introduced a framework, the Harmonised Mandatory Control System, in order to coordinate and harmonise the regulations of offshore chemicals within the convention area (Killaars et al., 2003). As a result numerous studies tend to develop new environmentally friendly components to reduce scale and corrosion (Yee, 2004, Martinod et al., 2008, De Souza and Spinelli, 2009, Sun et al., 2009, Kamal and Sethuraman, 2014 and Kumar et al., 2010).

To date most studies have focused on understanding and quantifying performance of either corrosion inhibitors or scale inhibitors (Darton, 1997, He et al., 1999, Palmer et al., 2004, Ghizellaoui et al., 2007, Sachin et al., 2007, Ketrane et al., 2009 and Hu et al., 2011). However, combined chemicals have been developed to increase injection efficiency and reduce the number of injection umbilicals (Choi et al., 2002, Jordan et al., 2003, Estievenart et al., 2004 and Touir et al., 2008). Collins et al. worked with polyaspartate based chemicals as scale and corrosion inhibitors (Collins et al., 2001). According to their results, polyaspartates were compatible with the production fluid and presented a high efficiency in reducing scale (in scale test) and corrosion (in corrosion test). Winning et al. tested two other types of blend composed of an amine base and a polymeric scale inhibitor (Winning et al., 2004). The additives were considered as acceptable for the environment and demonstrated a significant reduction in weld corrosion. In tests where pre-corrosion occurred, the corrosion rate dropped rapidly. It was postulated to be attributed to the presence of a scale active species which resulted in the break-down of the surface film induced during the pre-corrosion, leading to faster inhibition occurring (Winning et al., 2004). It is worth noting that such combined chemicals would typically be evaluated by focusing on scale efficiency in a scaling test or on corrosion efficiency during a corrosion test i.e. the two processes would be evaluated independently without affording consideration to any synergistic or antagonistic effects between corrosion and scale.

Surface scaling of pipework rarely occurs in environments where no corrosion exists, yet techniques used to develop and assess the performance of scale inhibitors tend to focus on assessing and reducing solely bulk/surface scaling, without affording consideration towards corrosion, whilst corrosion inhibitors are frequently evaluated in non-scaling environments.

With this in mind this current study combines the evaluation of both surface and bulk scaling processes with evaluation of scaling and corrosion processes. In this project, a calcium carbonate brine (with the presence of divalent ions) is tested in CO_2-saturated conditions in the absence and presence of combined inhibitors. Four important aspects of the scale/corrosion behaviour are examined which include (i) bulk scale precipitation, (ii) surface scaling, (iii) general corrosion and (iv) localised corrosion, permitting a full assessment of the chemical blends propensity to mitigate both scaling and corrosion.

2. Methodology for combined scale/corrosion assessment

2.1. Experimental setup

The setup used in this study is presented in Fig. 1 and consists of a 1 L glass beaker combined jar test/bubble cell. The compositions of the two brines (which were mixed to form a scaling brine) are presented in Table 1. The samples/working electrodes consisted of cylindrical carbon steel coupons (25 mm in diameter and 6 mm

thickness, exposed area of 4.9 cm^2) with the elemental composition provided in Table 2. Wires were soldered to the back of each sample to enable electrochemical tests to be performed before embedding the samples in a non-conducting resin using a standard embedding procedure. The samples were subsequently polished with silicon carbide grit paper to a 1000 grit finish, rinse with acetone and distilled water and dried prior to immersion in the corrosion/scaling brine. Each test commenced when Brine 1 and Brine 2 were mixed in the 1 L vessel in a 50/50 ratio in the presence of each steel sample.

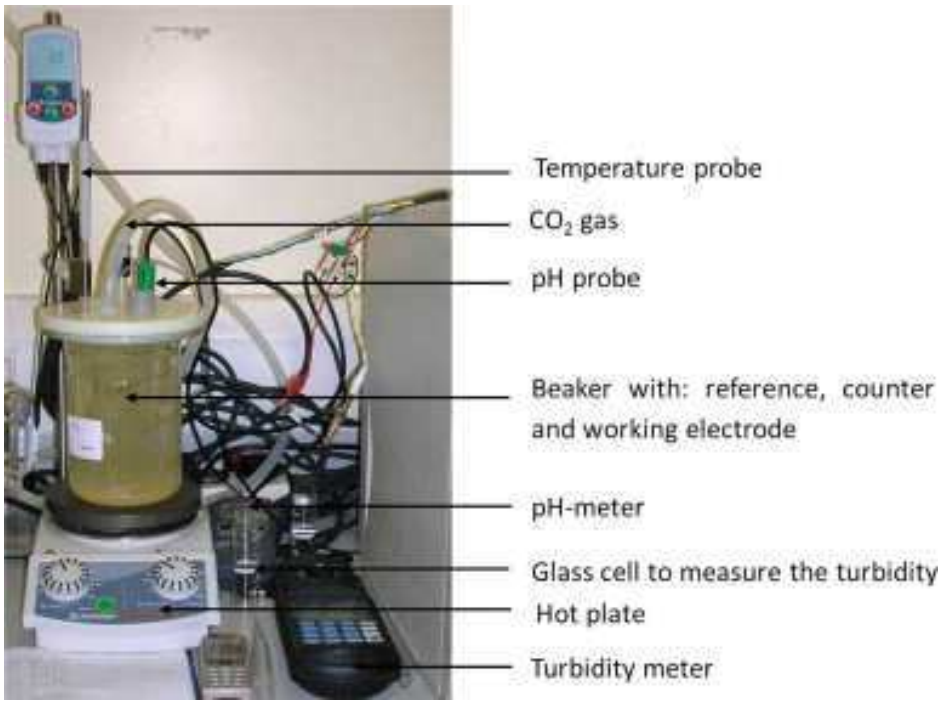

Fig. 1. Combined bulk jar/bubble cell test apparatus.

Table 1. Brine composition.

Brine 1 (mmol/l)		**Brine 2 (mmol/l)**	
Cl^-	137.5	Cl^-	1279.5
Ca^{2+}	71.6	HCO_3^-	71.4
Mg^{2+}	46.9	Na^+	1351.0
K^+	11.7		
Ba^{2+}	1.8		
Sr^{2+}	5.4		

Table 2. Measured chemical composition of X-65 mild steel (wt% balance being Fe).

C	Si	Mn	P	S	Cr	Mo	Ni	Ti
0.100	0.180	1.210	0.009	0.003	0.100	0.1600	0.070	<0.010

Scale in the bulk solution was assessed through manual measurement of the pH and the turbidity (in Formazin Attenuation Unit) using a pH/temperature metre and a colorimeter, respectively at regular time intervals. Corrosion was assessed using an electrochemical method involving a 3-electrode cell connected to a computer controlled potentiostat to conduct linear polarisation measurements (Klinghoffer, 1997). The sample formed the working electrode with a Ag/AgCl reference and a platinum counter electrode completing the remainder of the cell setup. The system was operated at atmospheric pressure with the partial pressure of CO^2 amounting to approximately 0.8 bar at 60 ℃. All tests were conducted in the absence of hydrocarbons as focus was directed here towards the simultaneous measurement of corrosion and scale processes. It is, however, appreciated that the presence of oil, could change the behaviour of the corrosion, scale and inhibitor efficiency but this lies beyond the scope of this work.

2.2. Scaling assessments

By monitoring the pH, the calco-carbonic equilibrium is followed and therefore the scaling process can be recorded. Information about the chemical reactions taking place in the cell can be yielded from the following equations:

$$CO_2+H_2O \leftrightarrows H_2CO_3 \quad (1)$$

$$H_2CO_3 \leftrightarrows HCO_3^- + H^+ \quad (2)$$

$$HCO_3^- \leftrightarrows CO_3^{2-} + H^+ \quad (3)$$

$$Ca^{2+} + CO_3^{2-} \leftrightarrows CaCO_3 \quad (4)$$

Dissolution of carbon dioxide in water leads to formation of carbonic acid which releases protons and forms carbonates. These subsequently react with the calcium ions present in the solution to form an insoluble precipitate (Becker, 1998).

Scaling occurs when the product of the concentrations of the calcium and bicarbonate ions exceed their solubility product (K_{sp}). The value of the solubility product is a function of temperature and ionic strength. The K_{sp} for $CaCO_3$ is 1.6×10^{-9} at 60 ℃ (Multiscale). The solubility of calcium carbonate has been shown to decrease with increasing temperature as $CaCO_3$ is a reverse solubility salt (Nancollas, 1979).

In general, temperature is a very important factor as it influences both the corrosion and scaling processes related to the formation of $FeCO_3$ and $CaCO_3$ on the surface as well as in the bulk phase (Garverick, 1994, Civan, 2007 and Zumdahl and Decoste, 2007). The supersaturation ratio (SR) in the tests performed here were calculated using the MultiScale software version 7.1 (Multiscale). With this specific software the main parameters such as temperature, pH, brine composition and alkalinity are considered. The calculations employ the Pitzer equation and are based on the thermodynamics of the system. The SR with respect to calcium carbonate was 36. All tests reported in this study were conducted at 60 °C which is a typical oil-field condition. The pH was monitored during the entire four hour experiment. All the values recorded were within the range of 6.6–5.6. For each test, the pH dropped by an average of 0.2 pH units over the course of the experiment, with a maximum drop of 0.5 being recorded within any single experiment.

Post-test surface analysis was performed using a Scanning Electron Microscope (SEM), to assess the extent of calcium carbonate deposition and the morphology of the deposited crystals. The samples were coated with gold in order to improve the electrical conductivity and to allow better image resolution under the SEM. The corrosion underneath the scale was evaluated after removing any precipitated products using an inhibited acid (Clarkes′ solution; 1000 ml of hydrochloric acid, specific gravity 1.19+20 g of Sb_2O_3+50 g of $SnCl_2$) (Singh and Kumar, 2003).

Inductively Coupled Plasma Atomic Emission Spectroscopy (ICP-AES) was implemented to enable quantification of the calcium carbonate present on the steel surface. Once the experiment was finished, the sample was immersed for 48 h into a 20 ml solution of 10% v/v acetic acid at a concentration of 17.5 mol/L (Stalker et al., 2004 and Jenkins and Cullion, 2009). The acetic acid dissolved the scale present on the surface of the metal and 10 ml of the solution produced was evaluated using ICP analysis. The results produced allowed the quantity of calcium to be determined from the surface (expressed in mg/cm2).

2.3. Corrosion assessments

A standard three-electrode electrochemical cell was used for corrosion rate measurements which were conducted using the Linear Polarisation Resistance (LPR) methodology. The 3-electrode cell consisted of the sample/working electrode, an Ag/AgCl reference and a platinum counter. The sample potential was scanned from 20 mV more negative than the open circuit potential (OCP) to 20 mV more positive than OCP, at a scan rate of 0.25 mV/s. The corrosion current density (icorr) was been calculated using the Stern–Geary equation (Eq. (5)). The anodic Tafel

constant (β_a) and the cathodic Tafel constant (β_c) were taken to be equivalent to 120 mV/decade.

$i_{corr}=1/2.303_{R_p\beta a\beta c}/(\beta a+\beta c)$ (5)

where R_p=polarisation resistance in Ω cm^2, which is the gradient of the plot of E vs. I over a small voltage perturbation from OCP (±20 mV).

The corrosion rates (CRs) have been calculated according to Eq. (6) (in mils per year or mpy) and converted into millimetres per year (mm/y) (1 mpy=0.0254 mm/y).

$CR=i_{corr}(K)1/\rho(\varepsilon)$ (6)

with K=conversion term=1.287×10^5 (eq.s.mils)/(C cm y), ρ=metal density=7.85 g/cm^3, ε=equivalent weight=27.9 g/eq.

Non-contact interferometry analysis was used to assess the deepest pits (Fig. 11), the extent of pitting (Fig. 12) and to provide 3D images of the analysed surface once the surface scale was removed using Clarkes′ solution (Fig. 17). The depth of the pits and their quantity depend on the processes occurring on the sample surface as a result of both corrosion and scale phenomena. Fig. 2 presents a schematic representation of a surface which has been subjected to pitting corrosion and general corrosion. The grey areas correspond to the material lost due to corrosion. According to the results found, it appears that a high percentage of pits exceed a depth of 3 µm and only a small percentage of the pits exceed 5 µm. Therefore, two thresholds (3 and 5 µm) were chosen for this study to enable the quantity of pits to be determined on the steel surface. In Fig. 3, the surface of a sample is presented where a threshold has been fixed. Only the grey regions (lost due to corrosion) are quantified (not the white regions). The higher the percentage of pit deeper than this threshold (grey regions), the lower the efficiency of the chemical at mitigating pitting corrosion. Such high levels of localised corrosion could be attributed to the heterogeneous or porous nature of the semi-protective film.

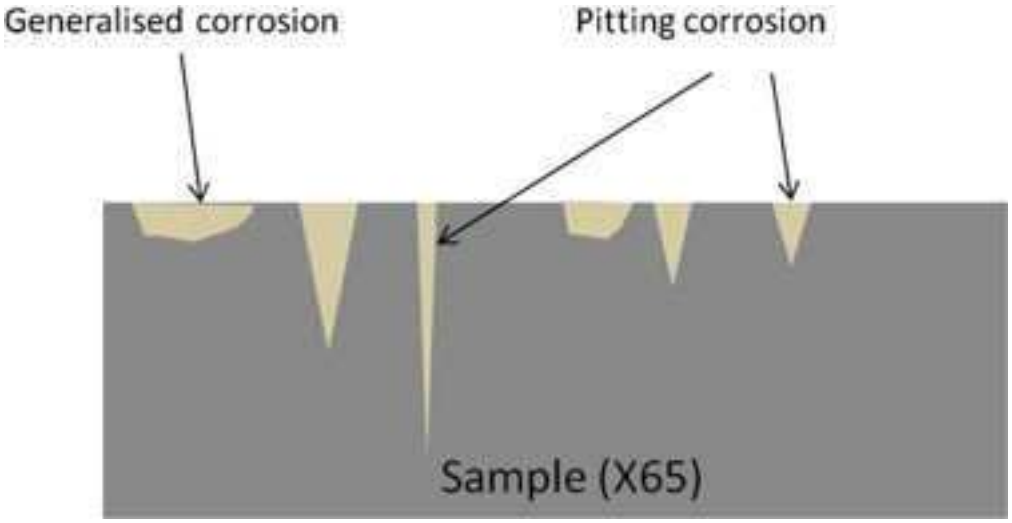

Fig. 2. Schematic representation of a sample after test.

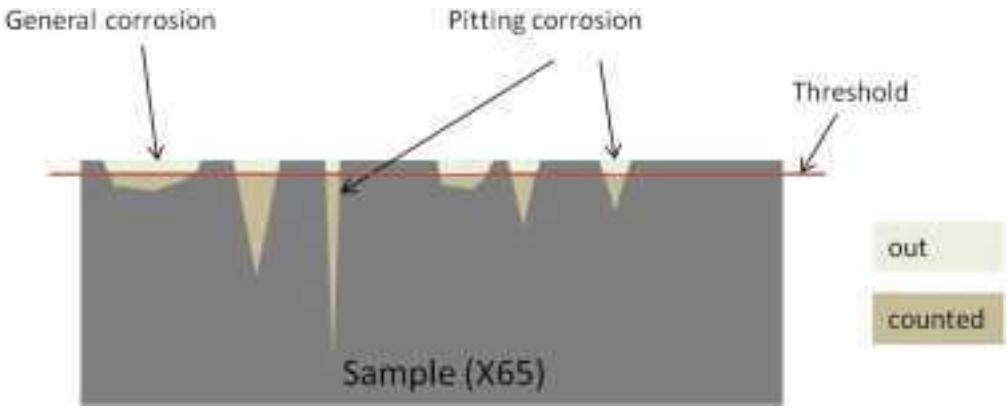

Fig. 3. Schematic representation of a sample after test with representation of a threshold.

The analysis performed enables the efficiency of each inhibitor (at concentrations of 2, 4 and 5 ppm) to be evaluated with respect to both general corrosion (from electrochemistry) and localised corrosion (from profilometry).

2.4. Combined inhibitor products

In this study, four combined inhibitors are assessed in their ability to control both scale and corrosion in an environment where both processes are occurring simultaneously. The generic descriptions of the four inhibitors are presented in Table 3. They have been named according to their composition; “MIQ” for Maleic acid, Imidazoline and Quaternary amine component, “PIQ” for Phosphonate, Imidazoline and Quaternary amine component, “MA” for Maleic acid and amine and “MPA” for Maleic acid, Phophate ester and Amine component. The structures of the main components of the inhibitors are presented in Fig. 4.

Table 3. Description of combined scale/corrosion inhibitors.

	MIQ	**PIQ**	**MA**	**MPA**
Scale	Maleic acid	Phosphonate	Maleic acid	Maleic acid
Corrosion	Imidazoline and quaternary amine	Imidazoline and quaternary amine	Amine	Phosphate ester and amine

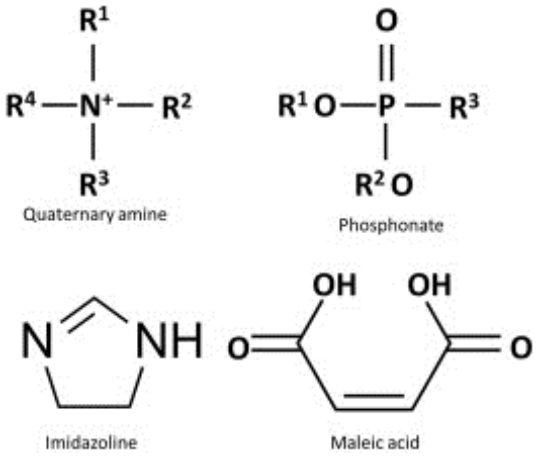

Fig. 4. Structure of the main component present in the inhibitor formulation.

It is worth noting that the main purpose of this paper is to compare the scaling and corrosion processes occurring on the steel surface in the presence of various combined inhibitors when both processes occur together. Therefore, the chemicals were first added at a low concentration of 5 ppm and efficiency of scaling (in the bulk solution and on the surface) and corrosion (as general and localised corrosion) have been assessed. Using such low concentration does not intend to be a direct link with the field, where it is appreciated that much higher inhibitor concentrations are used (25–50 ppm). Since it appeared that the processes were significantly reduced (with corrosion rate lower than 0.1 mm/y in two cases and more than 75% of bulk scale reduction), lower concentrations of inhibitor were chosen, in order to highlight a possible competition effect in reducing scale or corrosion. Inhibitors were then added at 4 and 2 ppm. As mentioned above, the paper is focussing on the mechanisms by which scale processes and corrosion processes interact; it is not intended to be a link to the field directly, nor to identify the inhibition processes of these chemicals at a molecular level.

A dilution of the inhibitor blend (1 ml of the blend in 1000 ml of distilled water) before adding the required amount of product in the experimental setup (5 ml of the blend for a 5 ppm concentration) to ensure accurate dosing of the chemical. The inhibitors were added directly after mixing the two brines.

3. Results and discussion

3.1. Non-inhibited tests

Scaling and corrosion measurements were initially assessed in the absence of inhibitor (baseline measurement). In Fig. 5(a), after a short induction time (T_{ind}), the turbidity starts to increase, revealing the formation of $CaCO_3$ in the bulk solution. At the same time, the corrosion rate of X65 decreases as a function of time and reaches a plateau close to 2 mm/y after 2 h of test, as shown in Fig. 5(b).

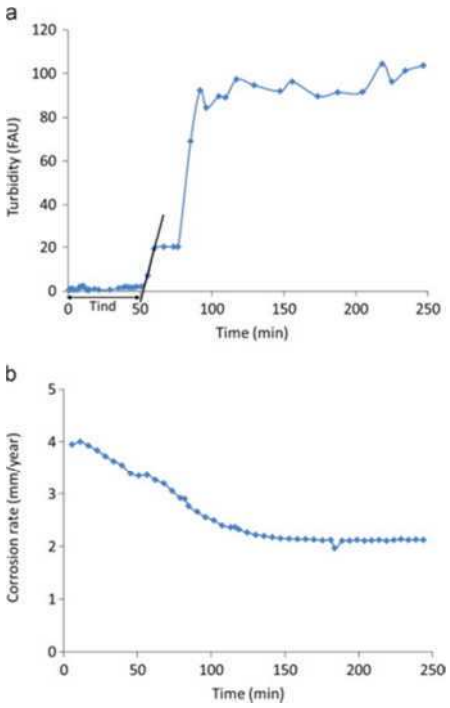

Fig. 5. Turbidity (a) and corrosion rate (b) as a function of time for non-inhibited experiment.

The aim of monitoring turbidity and corrosion rate as a function of time is to understand the precipitation processes occurring in the bulk solution. Furthermore, surface analysis is conducted (post-test analysis) in order to investigate which phenomena dominate on the surface. The SEM images of the surface in the absence of inhibitor are presented in Fig. 6. It is shown that a high mass of scale is deposited on the substrate. The presence of cubic crystals in Fig. 6 indicates the presence of calcite on the surface (Mullin, 2001).

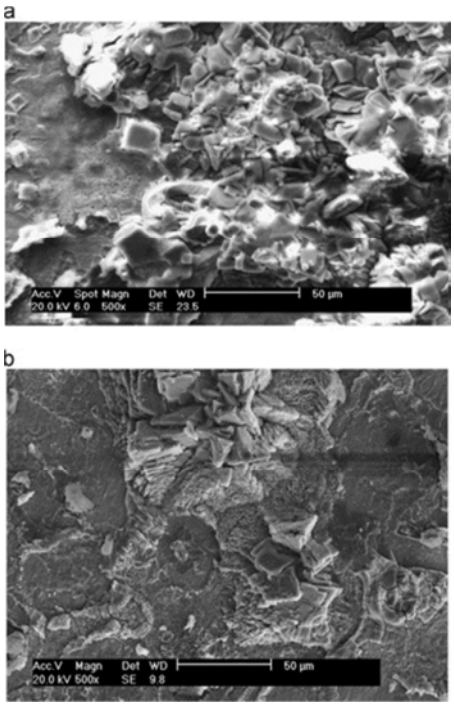

Fig. 6. SEM images of two different areas (a and b) of the non-inhibited sample.

Once the scale is removed from the surface, it is then possible to characterise the corrosion mechanisms which occurred on the surface of the sample. Surface analyses provide important additional information on localised corrosion that cannot be assessed by linear polarisation electrochemical measurements. 3D analysis of the surface shows pitting corrosion and corrosion occurring under the scale in blank conditions, as illustrated in Fig. 7.

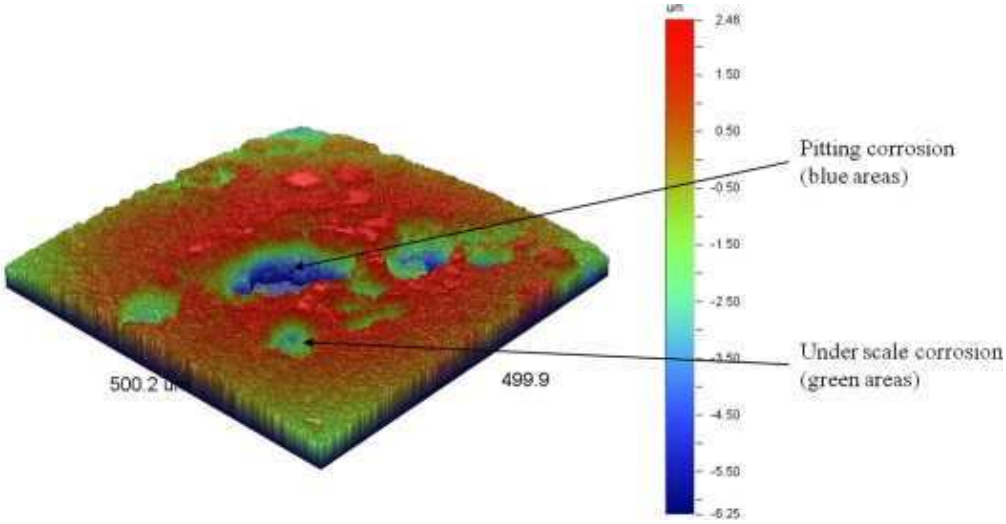

Fig. 7. 3D analysis of the non-inhibited sample.

3.2. Inhibited tests – bulk and general corrosion rate analysis

The four inhibitors MIQ, PIQ, MA and MPA were evaluated at concentrations of 2, 4 and 5 ppm. The results for the scale and the corrosion rates are presented in Fig. 8(a–f). Fig. 8(a), (c) and (e) shows that the turbidity values decrease when the concentration of the inhibitors was increased, as expected. Each inhibitor tested in these specific conditions is considered to be effective in reducing the turbidity value when compared with the non-inhibited case. In addition, the induction time is prolonged in the presence of inhibitors. The corrosion rate also decreased when the dosage of the chemicals increases (Fig. 8(b), (d) and (f)). At 5 ppm for MIQ, PIQ and MA the corrosion rate reaches a plateau before the fourth hour of the experiment. Conversely, MPA shows a slower trend to reach the plateau. Among all the tested inhibitors, PIQ appears to be the most effective in these conditions. This specific inhibitor reduces the turbidity and further decreases the corrosion rate much faster compared to the rest of the inhibitors (Fig. 8(f)), when applied at concentrations equal to or higher than 4 ppm.

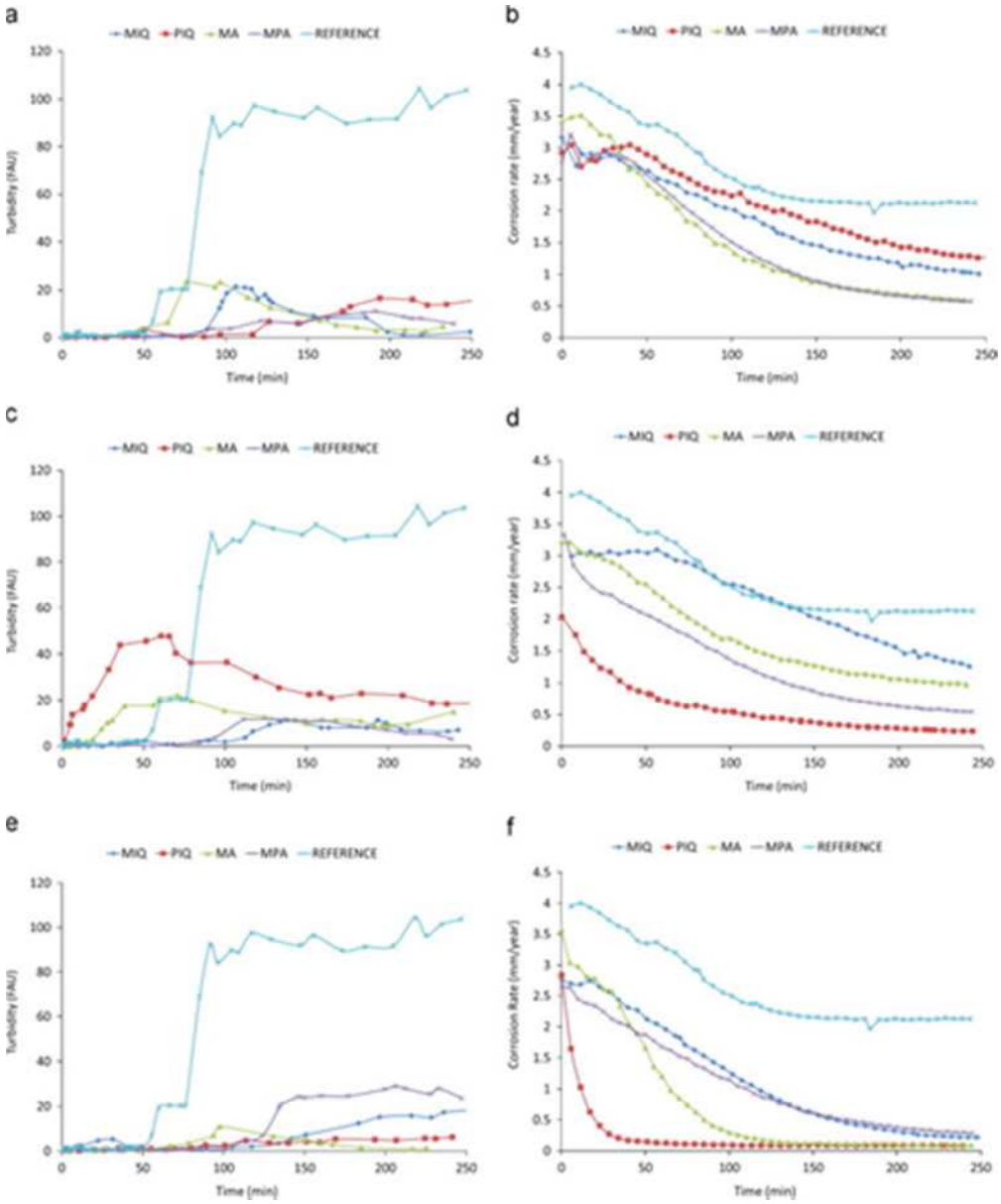

Fig. 8. Turbidity at (a) 2 ppm, (c) 4 ppm and (e) 5 ppm and corrosion rate at (b) 2 ppm, (d) 4 ppm and (f) 5 ppm as a function of time.

Table 4 illustrates the efficiency of the four chemicals on scale and corrosion. The efficiency (Eff) for each case has been calculated by considering the final values of turbidity and corrosion rate compared to the final values recorded with the non-inhibited case as

$$Eff(\%) = 100 \times \{(V_{f(ref)} - V_{f(test)})/V_{f(ref)}\} \qquad (7)$$

with $V_{f(ref)}$=final value of non-inhibited case and $V_{f(test)}$=final value of inhibited case.

Table 4. Efficiency (%) of the scale and the corrosion part.

	Inhibitor concentration (ppm)	Scale efficiency (%)	Corrosion efficiency (%)	Final corrosion rate (mm/y)
MIQ	2	98	53	1.01
	4	93	41	1.26
	5	84	90	0.21
PIQ	2	85	41	1.26
	4	82	89	0.24
	5	94	96	0.08
MA	2	95	72	0.60
	4	86	54	0.97
	5	99	96	0.09
MPA	2	95	73	0.57
	4	97	74	0.54
	5	77	87	0.28

By correlating the information from Fig. 8 and Table 4, Fig. 9 is obtained. It illustrates the efficiency of the reduction of scale (in the bulk solution) and corrosion (as general corrosion).

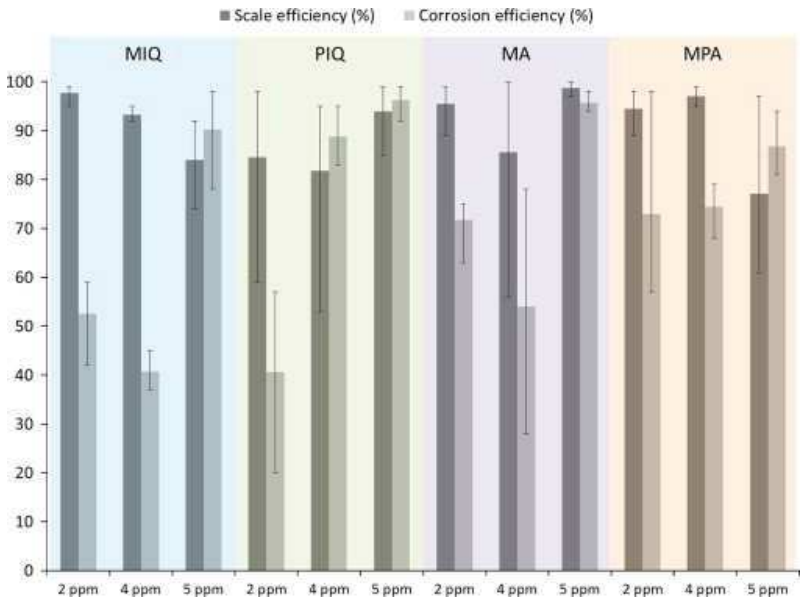

Fig. 9. Efficiency on scale and corrosion reduction (%) as a function of inhibitor concentration.

Fig. 8 and Fig. 9 and Table 4 suggest that 5 ppm is the most effective concentration, especially in terms of inhibiting corrosion at the tested conditions. 5 ppm is close to the absolute minimum concentration at which the products have an industrially useful effect. The scale and corrosion efficiencies when 2 and 4 ppm were added in the examined system were not consistent, indicating that there exists significant competition between scale and corrosion. The efficiency of each chemical for inhibiting scaling and corrosion is illustrated in Table 4. In terms of the mitigation of scale, it is conventionally accepted that an inhibitor is efficient when its reduces scale precipitation in the bulk phase by 75% (Sorbie et al., 2000 and Laing et al., 2003). In the current work, a reduction of 75% of bulk scale precipitation corresponds to turbidity values lower than 26 FAU. In terms of corrosion mitigation, the required efficiency is deemed to be achieved when the final corrosion rate is below the acceptable level of 0.1 mm/year (Garverick, 1994).

As shown in Table 4, in these experiments the applied chemicals are efficient at all concentrations in inhibiting the bulk scaling revealing efficiencies greater than 75%. An increase in the concentration of the inhibitor to 5 ppm improves the corrosion inhibition for all the chemicals, making this concentration the most efficient. However, only PIQ and MA can provide acceptable protection on the material by reducing the corrosion rate lower to 0.1 mm/y. For the chemicals PIQ and MA, the higher the concentration of the inhibitor, the lower the corrosion rate observed. This is not the case for the other two chemicals MIQ and MPA. Those two chemicals MIQ and MPA show the best reduction of the corrosion rate at 5 ppm, but on the other hand, it is at this concentration that the scale efficiency is the lowest. When using chemicals MIQ and MPA, at lower concentrations (2 ppm), the scale reduction is better but the corrosion efficiency is lower. When increasing the concentration to 4 ppm, the scale efficiency is quite similar but the corrosion efficiency dropped significantly. It seems to have a competition between scale and corrosion processes.

By comparing the results obtained from the inhibited tests with the non-inhibited ones, it is clear that every chemical reduces both scale and corrosion at any tested concentration in these specific tests. This analysis is further enhanced with the surface data (post-test analysis) presented in the next section.

3.3. Inhibited tests – post-test analysis

According to the different types of surface analyses performed in these specific experimental conditions, information regarding the mechanisms of scale and corrosion inhibition can be extracted. Fig. 10 presents the results of the ICP analysis for the concentration of calcium ion after dissolving the scale from the surface. The calcium concentration represents a quantitative measure of surface scale to complement the surface images shown later.

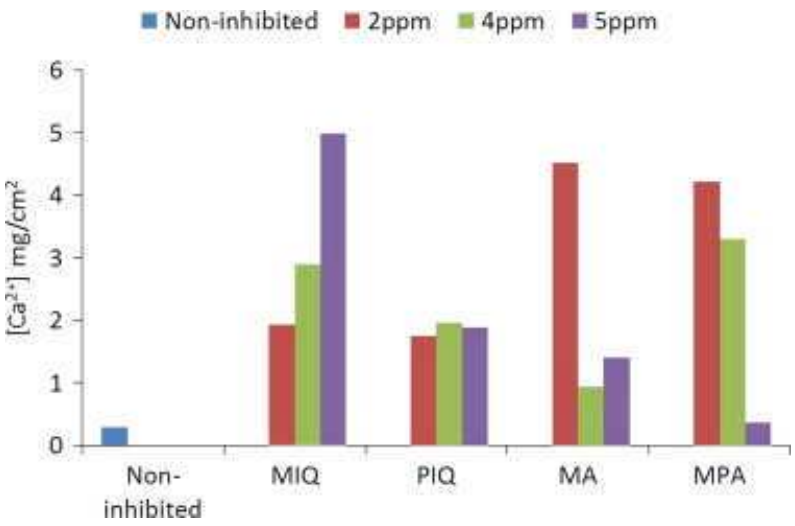

Fig. 10. ICP analysis of the amount of calcium dissolved with acetic acid from the surface of the sample.

By comparing the analysis of Ca^{2+} of the non-inhibited sample with the surface analysis of the inhibited sample, it appears that the amount of calcium is higher on the inhibited surfaces (Fig. 10). This is something unexpected if it is considered that the inhibitors reduce the amount of scale in the bulk solution. The inhibitors therefore tend to inhibit the formed scale in the bulk solution, but promote its formation on the surface.

Fig. 11 shows the deepest pitting corrosion encountered with interferometry measurements after the treatments with all the four inhibitors at different concentrations. It is clear that PIQ, which is considered as the most effective in controlling (i) the scale deposition of CaCO3 and (ii) the general corrosion rate, results in deeper pitting corrosion. MPA, which has the lowest corrosion efficiency, as shown in Fig. 8 leads to the lowest pitting corrosion. This suggests that inhibitor MPA does not interact significantly with the scale at the concentrations considered in this paper.

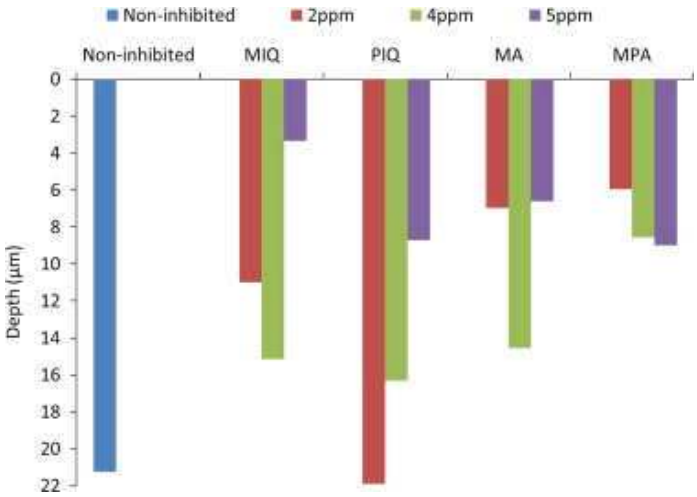

Fig. 11. Interferometry: surface analysis (deeper pitting observed for each sample).

In order to estimate the number of deep pits, the software used with the interferometry (Vision 32 analysis software) has been used to apply a threshold and to count only (as a percentage of missing metal) pits deeper than this established thresholds. For this study, two thresholds of 3 and 5 µm were applied (Fig. 12). As an example from Fig. 12, the non-inhibited test (reference) indicated that 45% of the pits on the surface are deeper than 3 µm and 10% are deeper than 5 µm. This type of analysis needs to be distinguished from the previous analysis (Fig. 12) which was showing the deeper pits encountered on the surface. Fig. 11 tends to correspond to a “qualitative analysis” and Fig. 12 to a “quantitative analysis”.

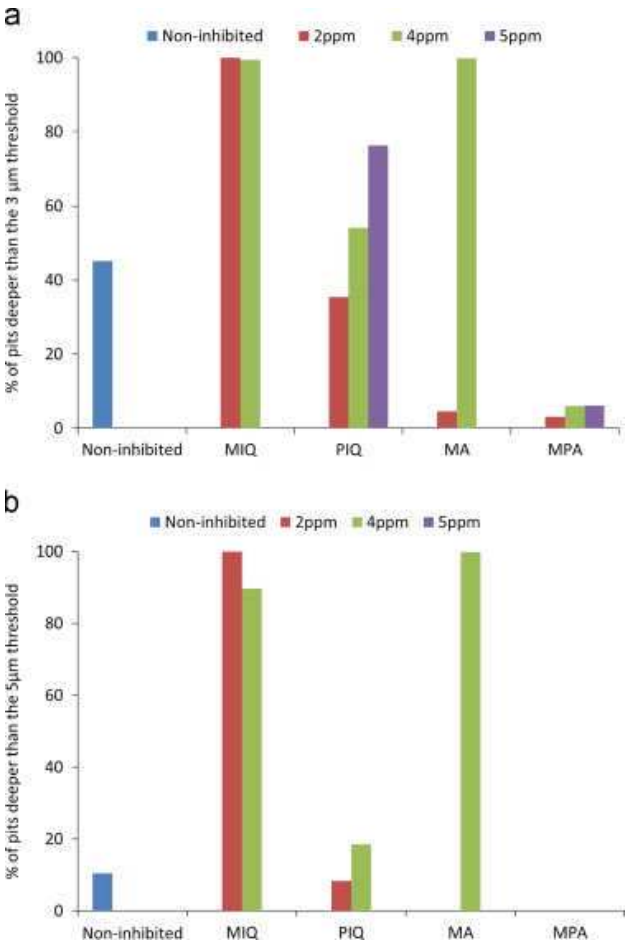

Fig. 12. Interferometry: surface analysis with (a) 3 µm and (b) 5 µm thresholds.

According to Fig. 12, different scenarios can be identified: (1) all the pits are below 3 µm (MIQ at 5 ppm and MA at 5 ppm), (2) only few pits are deeper compared to 3 µm with no pits deeper compared to 5 µm (MA at 2 ppm and MPA at 2, 4 and 5 ppm), (3) most of the pits have a depth between 3 and 5 µm (non-inhibited case and PIQ at 2, 4 and 5 ppm) and (4) finally, for three cases: MIQ at 2 and 4 ppm and MA at 4 ppm, the surface consists of numerous deep pits, with more than 95% of the pits exceeding the 5 µm threshold.

In order to characterise these cases, the software has been used to apply deeper thresholds. The aim was to find the threshold where 10% of the missing metal would be deeper than this threshold. The results are presented in Table 5.

Table 5. Threshold values of the cases where the surfaces present a lot a deep pits.

Chemical	Concentration (ppm)	Threshold (µm)	% Below
MIQ	2	6.6	~10
MIQ	4	5.7	~10
MA	4	8.8	~10

According to Table 5, with MIQ at 2 ppm, 10% of the pits encountered on the analysed surface are deeper than 6.6 µm. For MIQ at 4 ppm, 10% of the pits are deeper than 5.7 µm, and for MA at 4 ppm, 10% of the pits are deeper than 8.8 µm. The three thresholds found are less deep than 10 µm, and this suggests that only a few pits deeper than 10 µm are found on the analysed surface for these specific cases.

The results (related to both for the corrosion and the scale aspect phenomena) can then be linked to the 3D images from interferometry analysis (Fig. 17) and to the SEM images as shown in Fig. 13, Fig. 14, Fig. 15 and Fig. 16. SEM images of the non-inhibited and inhibited surfaces assess the effect of the chemicals on the $CaCO_3$ morphology.

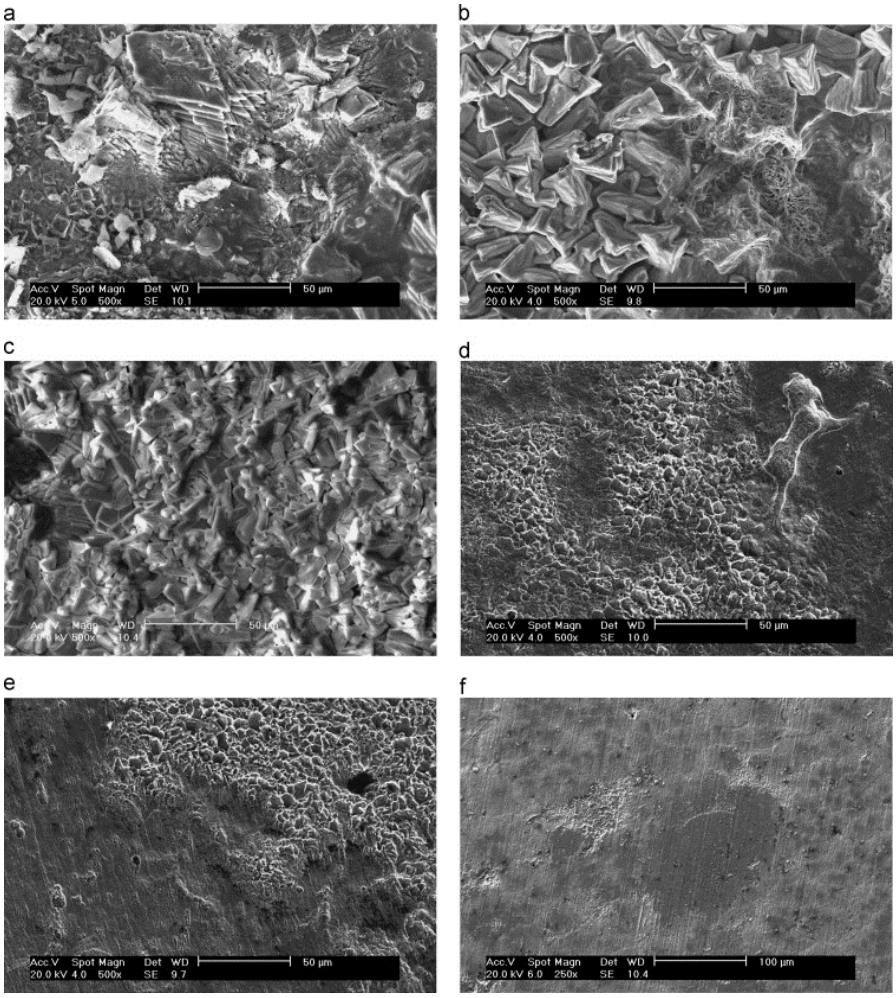

Fig. 13. SEM images of surface after treatment with MIQ: (a) scale-2 ppm, (b) scale-4 ppm, (c) scale-5 ppm. After removing scale (d) corrosion-2 ppm, (e) corrosion-4 ppm and (f) corrosion-5 ppm.

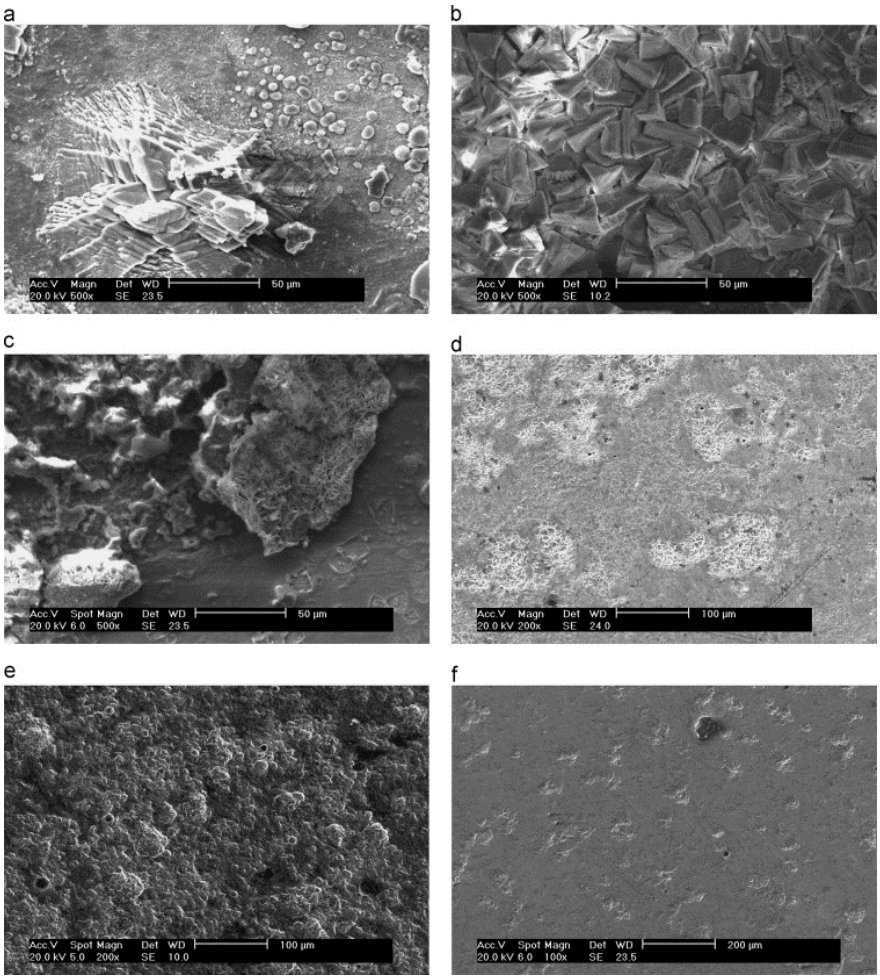

Fig. 14. SEM images of surface after treatment with PIQ: (a) scale-2 ppm, (b) scale-4 ppm, (c) scale-5 ppm. After removing scale (d) corrosion-2 ppm, (e) corrosion-4 ppm and (f) corrosion-5 ppm.

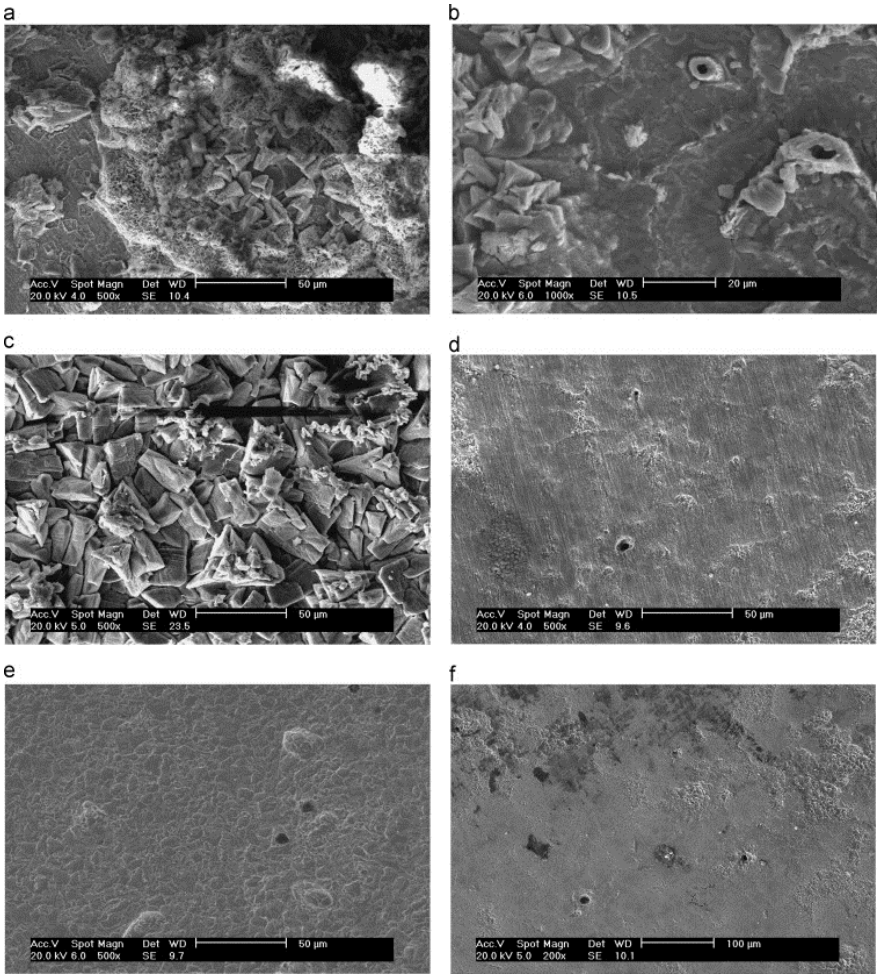

Fig. 15. SEM images of surface after treatment with MA: (a) scale-2 ppm, (b) scale-4 ppm, (c) scale-5 ppm. After removing scale (d) corrosion-2 ppm, (e) corrosion-4 ppm and (f) corrosion-5 ppm.

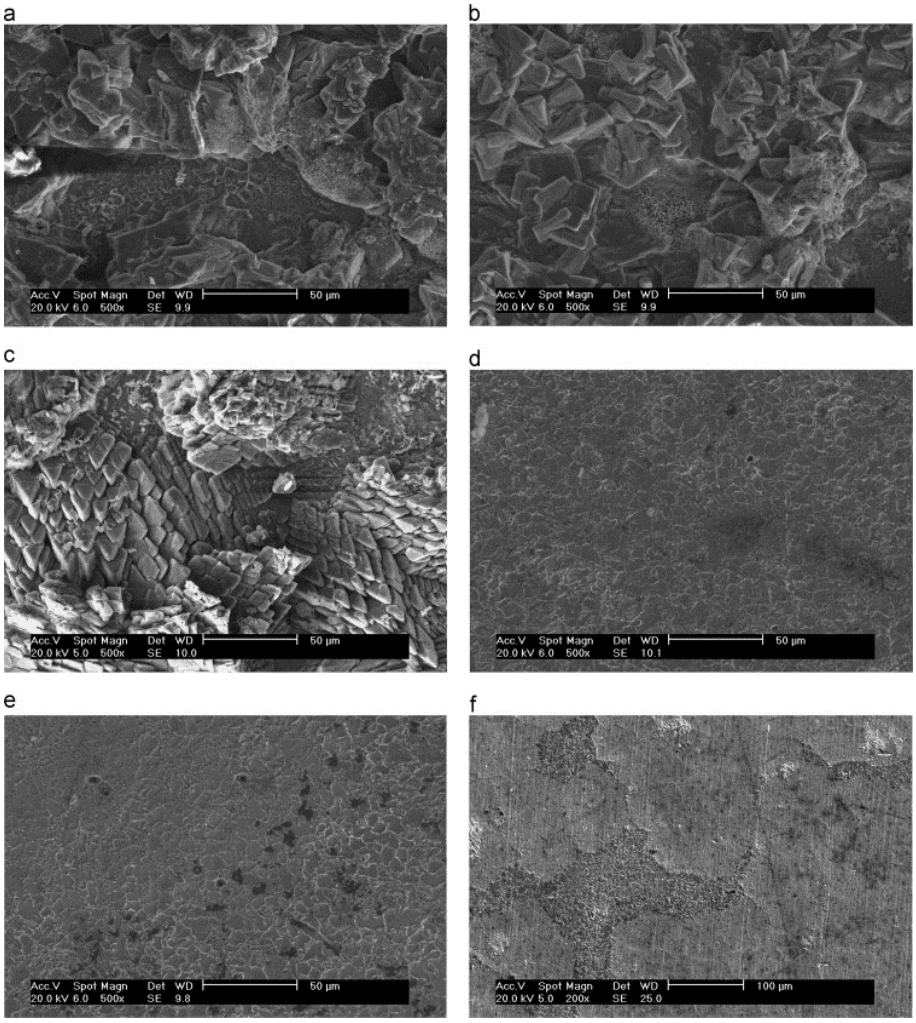

Fig. 16. SEM images of surface after treatment with MPA: (a) scale-2 ppm, (b) scale-4 ppm, (c) scale-5 ppm. After removing scale (d) corrosion-2 ppm, (e) corrosion-4 ppm and (f) corrosion-5 ppm.

All the SEM images show two types of corrosion: pitting corrosion (localised corrosion) and general corrosion. The general corrosion corresponds to underscale/underdeposit corrosion (highlighted using SEM, by marking an area on the sample before and after removing scale). The SEM images show the abundance of the calcium carbonate crystals and their morphology.

From the overall analysis, in these conditions of experiment, it can be extracted that, for MIQ (1) The higher its concentration, the more calcium present on the surface (Fig. 10) and the smaller is the depth of the pits. (2) The efficiency regarding the reduction of general corrosion is low in every case (Fig. 8) which is in agreement with the SEM images (Fig. 13(d)–(f)) showing a surface highly attacked by general corrosion. (3) There is a high number of shallow pits (depth between 2.5 and 10 µm, Fig. 11 and Fig. 12) especially at 2 and 4 ppm.

According to the above, the specific chemical does not promote the formation of an efficient protective layer in order to reduce the general corrosion rate. However, when increasing its concentration, it promotes scale formation on the surface, resulting in less severe localised corrosion (Fig. 17(a)).

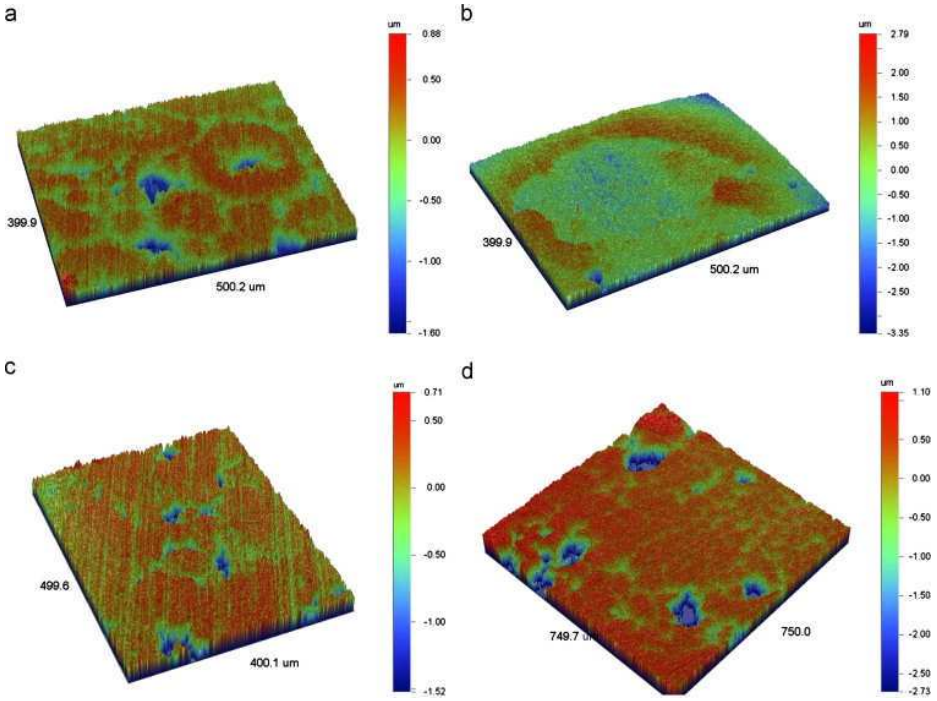

Fig. 17. 3D analysis of the surface after treatment with 5 ppm of inhibitor (a) MIQ, (b) PIQ, (c) MA and (d) MPA.

For PIQ some key points can be highlighted: (1) At 5 ppm, PIQ would tend to reduce general corrosion rate with a final CR below 0.1 mm/y (Fig. 8) rather than localised corrosion, since pits can be deeper than 20 μm (Fig. 12). (2) SEM analysis shows evidences of some generalised and localised corrosion but most of the surface does not appear to have suffered severe corrosion damage (Fig. 17(b)).

Therefore, the chemical has prevented the general corrosion of the surface, which is likely to be a result of the formation of a semi-protective film. However, this semi-protective film is not homogeneous and severe attack occurs at specific parts of the surface. For the concentrations of 2 and 4 ppm, PIQ presents a very low efficiency in reducing the scale formed in the bulk phase and reducing the general corrosion rate.

For MA, the results show that (1) The efficiency is the lowest at 4 ppm compared to 2 and 5 ppm, for both scale and corrosion processes (Table 4), as low scale reduction occurs in the bulk phase (Table 4) and small amount of calcium was detected on the surface (Fig. 10); (2) At 5 ppm final corrosion rate is below 0.1 mm/y; (3) At 4 ppm concentration, there is the presence of a significant amount of very deep pits (Fig. 11 and Fig. 12), since 99.8% of the pits are deeper than the 5 μm threshold as illustrated in Fig. 17(c). The surface has undergone severe localised attack.

When using MA, 5 ppm is the most effective concentration, leading to low general corrosion rate, shallow pits, prolonged induction time and low turbidity values.

For MPA (environmentally friendly chemical) it is seen that (1) the lower the concentration, the more calcium is present on the surface (Fig. 10); (2) at 5 ppm the efficiency is lowest compared to MIQ, PIQ and MA (Fig. 8) and the chemical needs 5 h to achieve a corrosion rate lower than 0.1 mm/y; and (3) only few shallow pits are

observed (for all the tested concentrations, Fig. 11 and Fig. 12) which are in agreement with the SEM pictures (Fig. 16).

MPA has a low efficiency in reducing general corrosion rate, but seems to prevent localised corrosion. By increasing its concentration to 5 ppm, scales develop in the bulk phase rather than on the surface and the pits are slightly deeper.

4. Conclusions

This paper presents initial results for a combined jar test/bubble cell methodology devised to assess the interactions between surface and bulk processes of scale and corrosion. The aim was to quantify the scale and corrosion phenomena when both were occurring in static conditions at 60 °C in the absence and presence of combined inhibitors. Four chemicals were evaluated through turbidity measurement, electrochemical methods and post-test surface analysis, in order to assess the interactions between scale in the bulk solution, scale on the surface of the metal, general and localised corrosion. The following conclusions can be made:

(1) In the bulk solution, the inhibitors act by increasing the induction time, but not necessarily by completely preventing scale formation; (2) Growth of calcium carbonate occurs in the bulk solution (turbidity measurements) and on the sample surface (SEM and ICP analysis); (3) The proportion of scale formed in the bulk phase or on the surface, varies according to the chemical type applied and its concentration; (4) High corrosion rates measured can be due to several reasons; one would be the very severe localised corrosion such as high pit depth (PIQ at 2 ppm). Also, a high corrosion rate could be due to a higher density of regions of localised attacks without creating considerably high pit depths (like MIQ at 2 and 4 ppm or MA at 4 ppm). (5) In some cases, the chemical seems to enhance the action against scale (MIQ at 4 ppm or PIQ at 2 ppm), and in other cases is more efficient in reducing the corrosion (MPA at 5 ppm or PIQ at 4ppm). Thus, there is a competition between the two phenomena. For the other cases, the interactions seem to be less evident and it is difficult to determine the straightforward performance of the chemical. (6) The corrosion rate can be reduced by the formation of a semi-protective film composed by products such as iron carbonate and/or incorporated elements, like calcium, which improve its protective properties.

Acknowledgements

The authors would like to thank the FAST III joint industrial project and the University of Leeds for the financial support.

References

[1] Becker, J.R., 1998. Corrosion and Scale Handbook. PennWell, Tulsa, Oklahoma.
[2] Chilingar, G.V.,Mourhatch, R., Al-Qahtani, G.D., 2008. Fundamentals of Corrosion and Scaling-For Petroleum and Environmental Engineers. Gulf Publishing Company, Houston, Texas.
[3] Choi, D.-J., You,S.-J., Kim, J.-G., 2002. Development of an environmentally safe corrosion, scale, and microorganism inhibitor for open recirculating cooling systems. Mater. Sci. Eng. A335 (1–2), 228–235.
[4] Civan, F., 2007.Inorganic scaling and geochemical formation damage, Reservoir Formation Damage, seconded. Gulf Professional Publishing, Burlington, pp. 407–467.
[5] Collins, I.R., Hedges, B., Harris, L.M., Fan, J.C. and Fan, L.D.G., 2001. The Development of a Novel Environmentally Friendly Dual Function Corrosion and Scale Inhibitor. SPE International Symposium on Oilfield Chemistry. Houston, Texas.
[6] Darton, E.G., 1997. Scale inhibition techniques used in membrane systems. Desalination 113(2–3), 227–229.
[7] De Souza, F.S., Spinelli, A., 2009. Caffeic acid as a green corrosion inhibitor for mild steel. Corros. Sci. 51(3),642–649.
[8] Estievenart, C., Fiaud, C., Kohler, N., Ropital, F., 2004. Mechanisms of Scale and Corrosion Inhibition by Polyaspartates. NACE International, New Orleans, LA (CORROSION2004).
[9] Frenier, W.W., Ziauddin, M., 2008.Formation, Removal, and Inhibition of Inorganic Scale in the Oilfield Environment. SPE Books.
[10] Garverick, L., 1994.Corrosion in the Petrochemical Industry. Materials Park, OH, ASM International.
[11] Ghizellaoui, S., Euvrard, M., Ledion, J., Chibani, A., 2007.Inhibition of scaling in the presence of copper and zinc by various chemical processes. Desalination 206 (1–3), 185–197.
[12] He, S., Kan, A.T., Tomson, M.B., 1999.Inhibition of calcium carbonate precipitation in NaCl brines from 25 to 90 1C. Appl. Geochem. 14(1), 17–25.
[13] Hu, X., Barker, R., Neville, A., Gnanavelu, A., 2011.Case study on erosion–corrosion degradation of pipework located on an offshore oil and gas facility. Wear 271 (9–10), 1295–1301.
[14] Jenkins, A., Cullion, P., 2009. High Temperature Environmentally Friendly Corrosion Inhibitor for Organic Acids. NACE International, Atlanta, Georgia.
[15] Jordan, M.M., Archibald, I., Donaldson, L., Stevens, K., Kemp, S., 2003.Deployment, Monitoring and Optimisation of a Combined Scale/Corrosion Inhibitor within a Subsea Facility in the North Sea Basin. International Symposium on Oilfield Chemistry. Houston, Texas, Society of Petroleum Engineers.
[16] Kamal, C., Sethuraman, M.G., 2012. Spirulina platensis – a novel green inhibitor for acid corrosion of mild steel. Arab. J. Chem. 5(2), 155–161.

[17] Ketrane, R., Saidani, B., Gil, O., Leleyter, L., Baraud, F., 2009. Efficiency of five scale inhibitors on calcium carbonate precipitation from hard water: effect of temperature and concentration. Desalination 249(3), 1397–1404.
[18] Killaars, J., Hall, J., Whitfill, D., 2003. Step change in development of environmentally responsible chemicals. In: Proceedings of the 10th Annual International Petroleum Environmental Conference.
[19] Klinghoffer, O., 1997.Techniques to assess the corrosion activity of steel reinforced concrete structures. Mater. Corros. 48(11), 776–777.
[20] Koch, G.H., Brongers, P.H., Thompson, N.G., 2001.Corrosion Costs and Preventive Strategies in the United States. NACE International, Houston, Texas.
[21] Kumar, T., Vishwanatham, S., Kundu, S.S., 2010.Alaboratorystudyonpteroyl-L-glutamic acid as a scale prevention inhibitor of calcium carbonate inaqueous solution of synthetic produced water. J. Pet. Sci. Eng. 71 (1–2), 1–7.
[22] Laing, N., Graham, G.M., Dyer, S.J., 2003.BariumSulphateInhibitioninSubsea Systems – The Impact of Cold Seabed Temperatures on the Performance of Generically Different Scale Inhibitor Species. International Symposium on Oilfield Chemistry. Houston, Texas.
[23] Lyons, W.C., Plisga, G.J., 1996. Standard Handbook of Petroleum and Natural Gas Engineering, 2nd ed. Elsevier, Houston, Texas.
[24] Martinod, A., Euvrard, M., Foissy, A., Neville, A., 2008.Progressing the under- standing of chemical inhibition of mineral scale by green inhibitors. Desalination 220(1-3), 345–352.
[25] Mullin, J.W., 2001.Crystallisation, 4th ed. Organic Process Research & Development, 6 (2), 201–202. Multiscale. NTNUSCALE Consult, EXPRO Norway.
[26] Nancollas, G.H., 1979. The growth of crystals in solution. Adv. Colloid Interface Sci. 10(1), 215–252.
[27] Nesic, S., Nyborg, R., Nordsveen, M., Stangeland, A., 2001. Mechanistic Modeling for CO2 Corrosion with Protective Iron Carbonate Films. NACE International, Houston, TX (CORROSION2001).
[28] Ospar, 2003.Strategies of the OSPAR Commission for the Protection of the Marine Environment of the North-East Atlantic.
[29] Palmer, J.W., Hedges, W., Dawson, J.L., 2004. Use of Corrosion Inhibitors in Oil and Gas Production:(EFC39).Maney Publishing, London, UK.
[30] Sachin, H.P., Achary, G., Naik, Y.A., Venkatesha, T.V., 2007.Protection of mildsteel against corrosion by polynitroaniline films. Mater.Chem.Phys.104(2–3), 422–428.
[31] Singh, D.D.N., Kumar, A., 2003.A Fresh Look at ASTMG1-90 Solution Recommended for Cleaning of Corrosion Products Formed on Iron and Steels. NACE International, Houston, Texas.

[32] Sorbie, K.S., Graham, G.M., Jordan, M.M., 2000. How Scale Inhibitors Work and How This Affects Test Methodology. Paper No.OFC-1 Presented at the 4th International Conference and Exhibition on Chemistry in Industry, Manama, Bahrain.
[33] Stalker, R., Graham, G.M., Simpson, C., 2004. The Impact of Inorganic Scale Deposits and Their Removal on General CO2 Corrosion Rates and Corrosion Inhibitor Performance. SPE International Symposium on Oilfield Corrosion. Aberdeen, United Kingdom.
[34] Sun, W., Nesic, S., 2008.Kinetics of Corrosion Layer Formation: Part1 – Iron Carbonate Layers in Carbon Dioxide Corrosion. Corrosion 64(4), 334–346.
[35] Sun, Y., Xiang, W., Wang, Y., 2009. Study on polyepoxysuccinic acid reverse osmosis scale inhibitor. J. Environ. Sci. 21(Suppl.1), S73–S75.
[36] Touir, R., Cenoui, M., ElBakri, M., EbnTouhami, M., 2008. Sodium gluconate as corrosion and scale inhibitor of ordinary steel in simulated cooling water. Corros. Sci. 50(6), 1530–1537.
[37] Touir, R., Dkhireche, N., EbnTouhami, M., Lakhrissi, M., Lakhrissi, B., Sfaira, M., 2009. Corrosion and scale processes and their inhibition in simulated cooling water systems by monosaccharides derivatives: PartI – EIS study. Desalination 249(3), 922–928.
[38] Winning, I.G., Mcnaughtan, D., Bretherton, N., 2004. Evaluation of Weld Corrosion Behavior and the Application of Corrosion Inhibitors and Combined Scale/ Corrosion Inhibitors. NACE International, Houston, Texas.
[39] Yee, Y.J., Green Inhibitors for Corrosion Control: A Study on the Inhibitive Effects of Extracts of Honey and Rosmarinus Officinalis L. (Rosemary), 2004, M.Scthesis, University of Manchester Institute of Science and Technology, Corrosion and Protection Centre.
[40] Zumdahl, S.S., Decoste, D.J., 2007.Introductory Chemistry. Cengage Learning, Belmont, CA, Brooks/Cole. L. Sanders et al./ Journal of Petroleum Science and Engineering 118 (2014) 126–139 139